IL6 and CXCL8 mediate osteosarcoma-lung interactions critical to metastasis

Supplemental Information – Xenograft Biology

A detailed understanding of the interactions of human and murine cytokines/chemokines on the receptors of the other species is essential to the understanding and interpretation of results such as those presented here. In these studies, the biology of IL6 is particularly important to facilitating accurate interpretation. Human and murine IL6 cytokines are homologous, as are their receptors. However, it has been reported that, while human IL6 very effectively activates the murine receptor, the reverse is not true (1). Therefore, while human tumor cells in a xenograft model can activate murine "host" cells, IL6 produced by the murine host cells will not activate the IL6 receptor complex in the human tumor cells. Given the single previous publication demonstrating this concept, we sought to validate this concept before accepting it as true. Our results (**Supplemental Figure 7**) were consistent with those reported previously.

The study of CXCL8 biology using murine models is likewise not straightforward. Mice do not make CXCL8, and there is no obvious murine homolog for that cytokine. The biology of murine CXCL8 as it relates to analogous human chemokine biology has been studied extensively (reviewed in (2)). Most agree that related cytokines (most notably KC and MIP-2) serve as functional orthologs of human CXCL8 in mice. These chemokines also signal through murine CXCR1 and 2. Importantly, human CXCL8 activates murine CXCR1/2 and elicits biological responses similar to those seen in humans (2). Conversely, murine KC and MIP-2 can activate the human CXCR1 and 2 and elicit responses similar to activation with CXCL8. Importantly, we note that marked effects were seen when we knocked down IL-8 in the human tumors implanted

into mice (**Figure 5**). For these reasons, we feel that studies of IL-8 biology can be undertaken

in mice, though results should be interpreted with caution.

1.   van Dam M, Müllberg J, Schooltink H, Stoyan T, Brakenhoff JP, Graeve L, et al. Structure-function analysis of interleukin-6 utilizing human/murine chimeric molecules. Involvement of two separate domains in receptor binding. J Biol Chem. 1993;268:15285–90.
2.   Singer M, Sansonetti PJ. IL-8 Is a Key Chemokine Regulating Neutrophil Recruitment in a New Mouse Model of Shigella-Induced Colitis. J Immunol. 2004;173:4197–206.
3.   Singh S, Sadanandam A, Varney ML, Nannuru KC, Singh RK. Small Interfering RNA-mediated CXCR1 or CXCR2 Knock-Down Inhibits Melanoma Tumor Growth and Invasion. Int J Cancer. 2010;126:328–36.
4.   Root DE, Hacohen N, Hahn WC, Lander ES, Sabatini DM. Genome-scale loss-of-function screening with a lentiviral RNAi library. Nat Methods. 2006;3:715–9.

Supplemental Table 1. qRT-PCR Primer Sequences.

Target	Amplicon	Forward Sequence	Reverse Sequence
Candidate genes			
ADAM28	105	AAA GTA CGG GTA CTG TCG CA	GGC AAA TTA TCC GAC CCA CC
AIF1	111	AGG AAA AGC TTT CGG ACT GC	TTG GAG GGC AGA TCC TCA TC
BMP2	98	CTT TCA ATG GAC GTG TCC CC	GCA GCA ACG CTA GAA GAC AG
BMP3	117	ATC TCC CCC AAG TCC TTT GAT	CCC CAC AGC TCT CAC TAT ACT C
BMP6	116	GAC ATG GTC ATG AGC TTT GTG A	ACC ACC TCA CCC TCA GGA AT
CCL21	108	TGG CCT CTT ACT CAC CCT CT	CTC CAT CAC TGC CTT GGG TC
CCR7	86	TTC CTG TGT GGT TTT ACC GC	AAT GAC AAG GAG AGC CAC CA
CD37	97	TGA CAA GAC CAG CTT CGT GT	GCC CAT GGT GAA GAT TCC TG
CLEC12A	114	CTC TCC ACC ACA CTG CAA AC	GCT GTC CTT ATG CCA AAT CCA
CLEC5A	78	GTG GCG TTG GAT CAA CAA CT	CCA ATG GTC GCA CAG TTG AA
CTGF	121	AAG GGC AAA AAG TGC ATC CG	ATC GGC CGT CGG TAC ATA CT
CXCL12	123	GTG CAT TGA CCC GAA GCT AA	GTT TCA GAG CTG GGC TCC TA
CXCL16	113	CCT GCT GGT GTA CCT GAC TC	TCA TGA ACT GAA CCG ATG GC
CXCL2	78	CAG AAA GCT TGT CTC AAC CCC	GCC ACC AAT AAG CTT CCT CC
CXCR2	123	CCC AGC ACT CAT CCC AGA ATC	GTT GCA GGG GGA AAT CCA G
CXCR4	89	GAG AAC CAG CGG TTA CCA T	CAT GGA GTC ATA GTC CCC TGA G
DLL1	81	GGG AGA AAG TGT GCA ACC C	CAT GCT GCT CAT CAC ATC CAG
dNP63	99	ACC TGG AAA ACA ATG CCC AGA	ACG AGG AGC CGT TCT GAA TC
EREG	106	ACA GGC AGT CCT CAG TAC AAC	TTG AGC ACA CGT GGA TTG T
PDIA6	115	TCC ATC GAA TTT CAA CCG AGA AG	TGC TGC TTT CTT CCA TTC TGG
FGF18	76	CCA GCA AGG AGT GTG TGT TC	CCG GAG TAC TTA GCC GAC AT
FGL2	124	GCT GGT GGT TTG ATG CAT GT	CCA GGG TGT GCC TCA CTT AC
FGFR2	118	CTG CCC TAC CTC AAG GTT CT	CCG CCA GCA CGT ATA TTC C
FHL2	111	CGA ATC CGG TGC GAG AC	TTG CAA TGG TGG CAG TCA AAG
FSCN1	107	AAG GAC GAG CTC TTT GCT CT	TGA TTG GCA GAC AGG TCC AT
GH1	87	CCC AGA CCT CCC TCT GTT TC	GGA GCA GCT CTA GGT TGG AT
HCST	105	CCA TCT GGG TCA CAT CCT CTT	CCT GAA GTG CCA GGG TAA AAG
ID1	99	GTT CCA TTT TCC GTA TCT GCT TC	CCA CTG GCG ACT TTC ATG AT
IFNGR1	124	ATG GAG ACG AGC AGG AAG TC	TCA TCT TCC TTC TGC GTG AGT
IGF1	90	ATC AGC AGT CTT CCA ACC CA	GAA GAG ATG CGA GGA GGA CA
IL13RA2	110	GCT GGG AAG GTG AAG ACC TA	TGG CTT ACG CAA AAG CAG AC
IL6	108	CAA CCT GAA CCT TCC AAA GAT G	ACC TCA AAC TCC AAA AGA CCA G
IL6ST	72	TCC ATC CCA TAC TCA GGC T	CCA TTG GCT TCA AAA GGA GGC
CXCL8	94	CAA TGC GCC AAC ACA GAA AT	TCT CCA CAA CCC TCT GCA CC
ITGB2	106	CAC ACC GAG GGA CAT GCT G	GCT GAC CTT GAA CTT CGT GC
JAG1	71	TCG TGC TGC CTT TCA GTT TC	ATT ACT GGA ATC CCA CGC CT
LITAF	115	ATG GGA AGG GCA TGA ATC CT	CGG TCC AAA AAG GTG ATG GG

| MAN1A1 | 93 | ATG GCC CAA CAC TAC CTT GA | AGC TTC TGG TCC CAG TTT CA |
MMP1	122	TTC CCA GCG ACT CTA GAA ACA	ACT GGG CCA CTA TTT CTC CG
MMP2	90	TGA TCT TGA CCA GAA TAC CAT CGA	GGC TTG CGA GGG AAG AAG TT
MMP9	120	ACG TCT TCC AGT ACC GAG AG	GCA GGA TGT CAT AGG TCA CG
NOTCH1	83	CTG GAC CAG ATT GGG GAG TT	GCA CAC TCG TCT GTG TTG AC
NOTCH2	108	ATT TCA AGT GCT CTT GCC CA	TAT CCA TGC ACT GAC CAC CA
OGFRL1	112	AAA TGT TGC TCG GGC TGT TA	ATA TCC AAG CTC ACC AAG GCT
PTH	73	AAT GGC TGC GTA AGA AGC TG	GCA TCT CTG GGA GCT AGA GG
PTHLH	109	AAG GTG GAG ACG TAC AAA GAG C	CAG AGC GAG TTC GCC GTT T
RARRES3	84	CTG TGA GCA CTT TGT CAC CC	GCC ACA CCA ACT TCA ACC TT
S100A8	99	TCA GCT GTC TTT CAG AAG ACC T	CTT GTG GTA GAC GTC GAT GAT
S100A9	100	TCA AAG AGC TGG TGC GAA AA	GCA TTT GTG TCC AGG TCC TC
SEMA4A	75	CCC CCT TCT TCT TTC TCC TGA AT	TGA ACC AGC CAC AGT GGG AA
SPP1	110	TCA CCT GTG CCA TAC CAG TT	AGA TGG GTC AGG GTT TAG CC
TGFB1	92	CTT CCA GCC GAG GTC CTT	CCC TGG ACA CCA ACT ATT GC
THBD	108	ACA TCC TGG ACG ACG GTT TC	CGC AGA TGC ACT CGA AGG TA
TLR4	97	TGC GTG AGA CCA GAA AGC TG	GCT CCG GAG TCT GAA AGC TC
TNC	115	GGA AAC TGC CCT CCT TAC CT	GGT GGT ATC TGG ACC CAC AA
TNF	112	AGC CTG TAG CCC ATG TTG TA	AGC TGG TTA TCT CTC AGC TCC
VCAM1	125	ACA ATG AAT CCT GTT AGT TTT GGG	TGA ATC TCT GGA TCC TTA GGA AAA
Internal Controls			
ACTB	76	ACA GAG CCT CGC CTT TGC	CGC GGC GAT ATC ATC ATC CA
GAPD	117	TTG AGG TCA ATG AAG GGG TC	GAA GGT GAA GGT CGG AGT CA
PGK1	108	CTT GGG ACA GCA GCC TTA AT	CAA GCT GGA CGT TAA AGG GA
RPL13A	93	GGC CCA GCA GTA CCT GTT TA	AGA TGG CGG AGG TGC AG

Supplemental Table 2. shRNA targeting sequences.

IL6 sh2 F	CCG GGC AGG CAC TTA CTA CTA ATA ACT CGA GTT ATT AGT AGT AAG TGC CTG CTT TTT G
IL6 sh2 R	AAT TCA AAA AGC AGG CAC TTA CTA CTA ATA ACT CGA GTT ATT AGT AGT AAG TGC CTG C
IL8 sh3 F	CCG GCA AGA GAA TAT CCG AAC TTT ACT CGA GTA AAG TTC GGA TAT TCT CTT GTT TTT G
IL8 sh3 R	AAT TCA AAA ACA AGA GAA TAT CCG AAC TTT ACT CGA GTA AAG TTC GGA TAT TCT CTT G
CXCL1/2 sh1 F	CCG GCC CTT CTA TAG TGG CAT CCT GCT CGA GCA GGA TGC CAC TAT AGA AGG GTT TTT G
CXCL1/2 sh2 R	AAT TCA AAA ACC CTT CTA TAG TGG CAT CCT GCT CGA GCA GGA TGC CAC TAT AGA AGG G
gp130 sh2 F	CCG GAC CGT GCA TCG CAC CTA TTT ACT CGA GTA AAT AGG TGC GAT GCA CGG TTT TTT G
gp130 sh2 R	AAT TCA AAA AAC CGT GCA TCG CAC CTA TTT ACT CGA GTA AAT AGG TGC GAT GCA CGG T
Scramble sh F	CCG GCC TAA GGT TAA GTC GCC CTC GCT CGA GCG AGG GCG ACT AAC CTT AGG TTT TTT G
Scramble sh R	AAT TCA AAA ACC TAA GGT TAA GTC GCC CTC GCT CGA GCG AGG GCGA CTT AAC CTT AGG

The above oligos were designed for overhang cloning after annealing of forward and reverse sequences into tet-pLKO-neo (a gift from Dmitri Wiederschain, Addgene plasmid # 21916) or tet-pLKO-puro (a gift from Dmitri Wiederschain, Addgene plasmid # 21915) plasmids. The sequences targeting CXCL1/2 were derived from Singh et al (3). All other shRNAs were designed using sequences published by the Broad Institute's Genetic Pertubation Platform (4). All oligos selected resulted from validation of target sequences using RNAi and selecting for efficacy and low levels of off-target effects (as measured by effects on the other receptors/cytokines/chemokines).
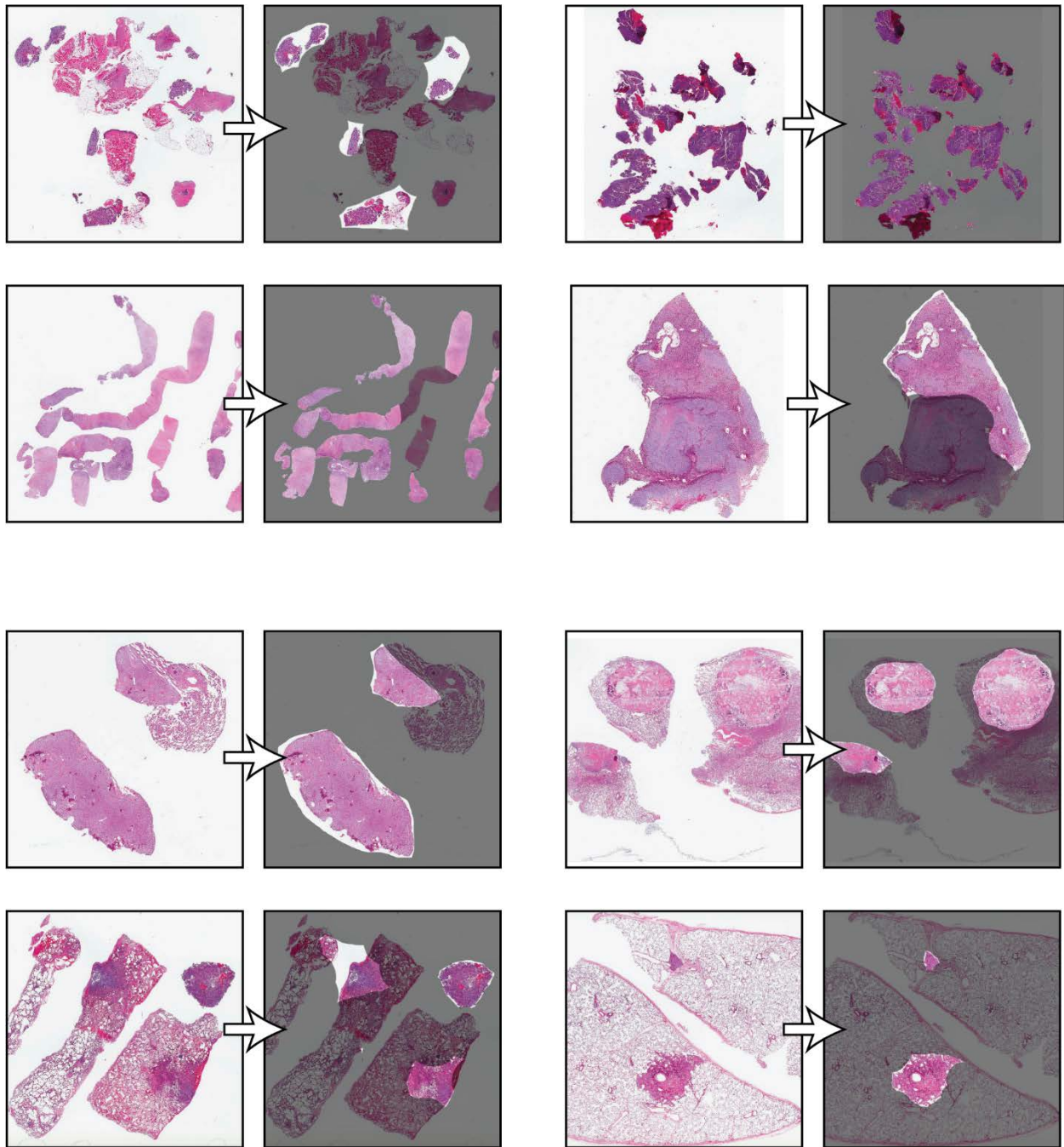
Supplemental Figure 1. Representative gross sections from primary and metastatic tumor samples. H&E stained slides from center sections (11 adjacent sections cut, section 6 processed for H&E shown) show specimens taken from primary tumor biopsies (top four) and lung metastases (bottom four). Tissues masked in the right-side images were dissected away on the slides prior to processing.
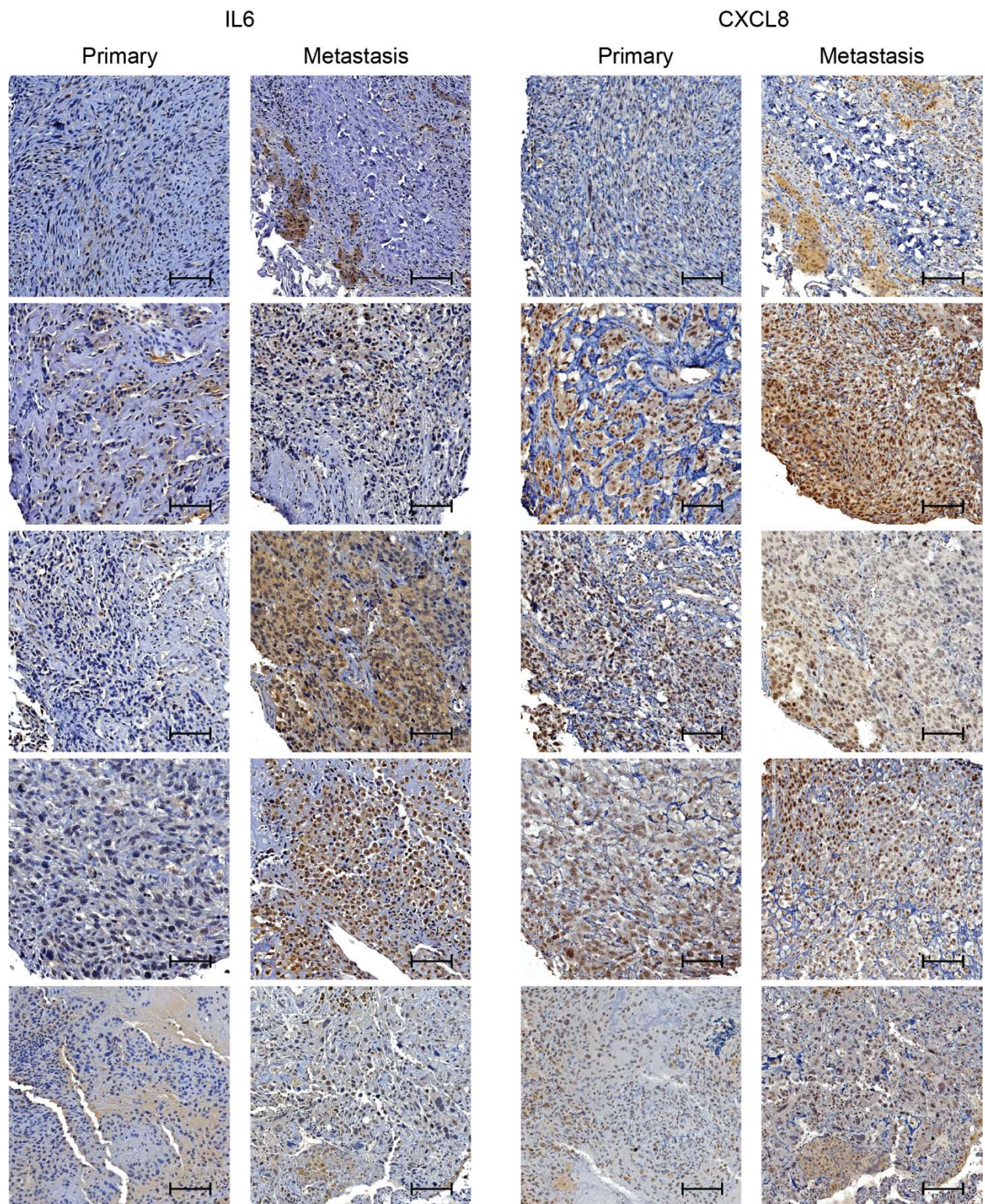
Supplemental Figure 2. Additional IHC on patient samples from primary tumors and lung metastasis confirms changes in the patterns of IL6 and CXCL8 expression. Additional

examples of IHC from patient primary and metastasis tumors stained by immunohistochemistry for IL6 and CXCL8. Each row represents samples from an individual patient. The columns on the left show primary and metastasis tumors stained for IL6. Panels in the right two columns show the same samples stained for CXCL8. Scale bars represent 100 µm.
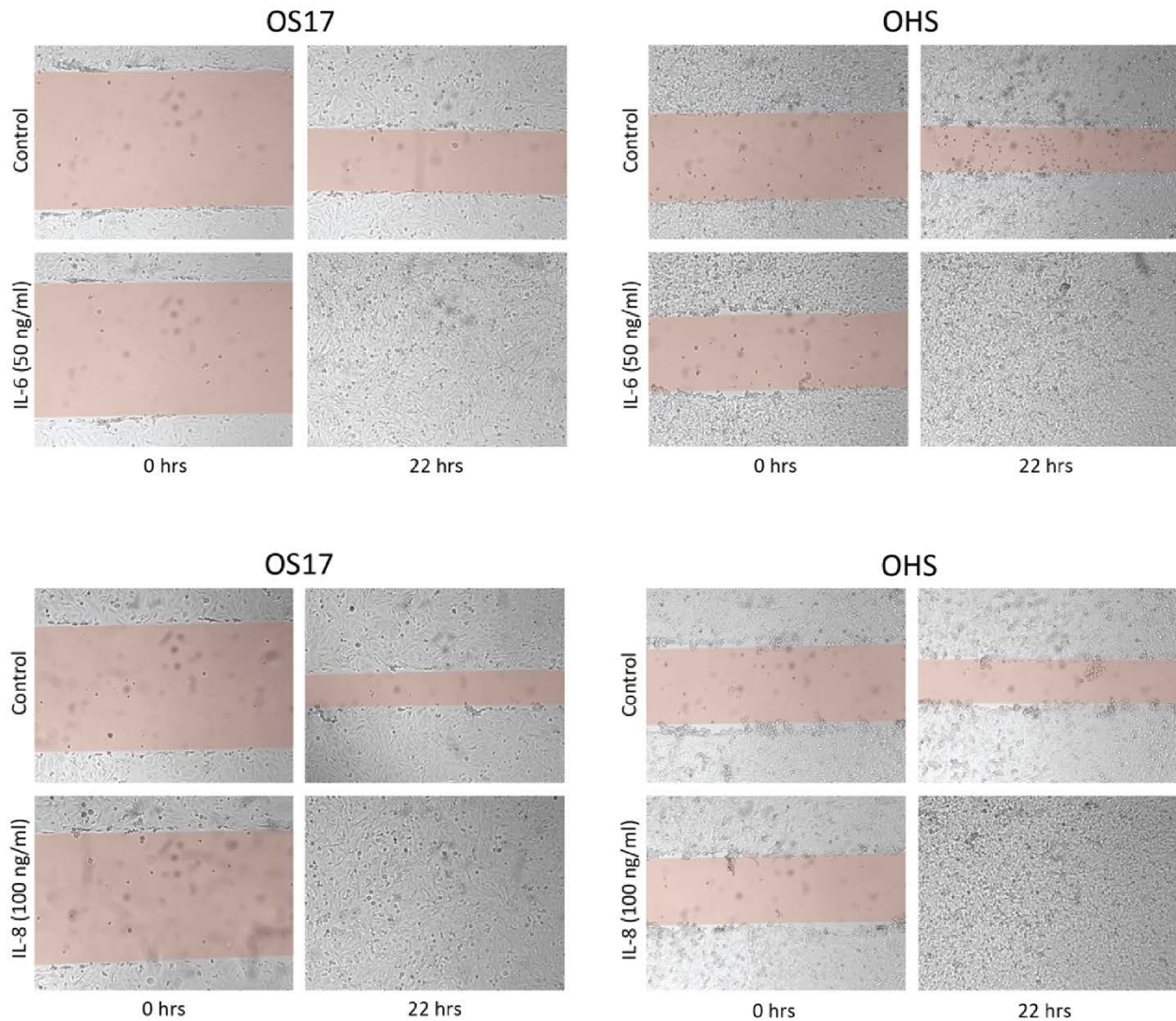
Supplemental Figure 3. IL6 and CXCL8 (IL8) stimulate chemokinesis in both highly metastatic and poorly metastatic OS cells. OS-17 or OHS cells were cultured in 96-well flat-bottomed plates, then "wounded" with a standardized instrument (IncuCyte® Scratch Wound Cell Migration and Invasion System). Serial images were subsequently taken to observe and quantify the rate at which the "wound" closed. Representative images from each data set are shown above.

Vehicle   30 mg/kg DF2156A, 24 hours

Brown = pFAK

Vehicle   10 mg/kg sc144, 24 hours
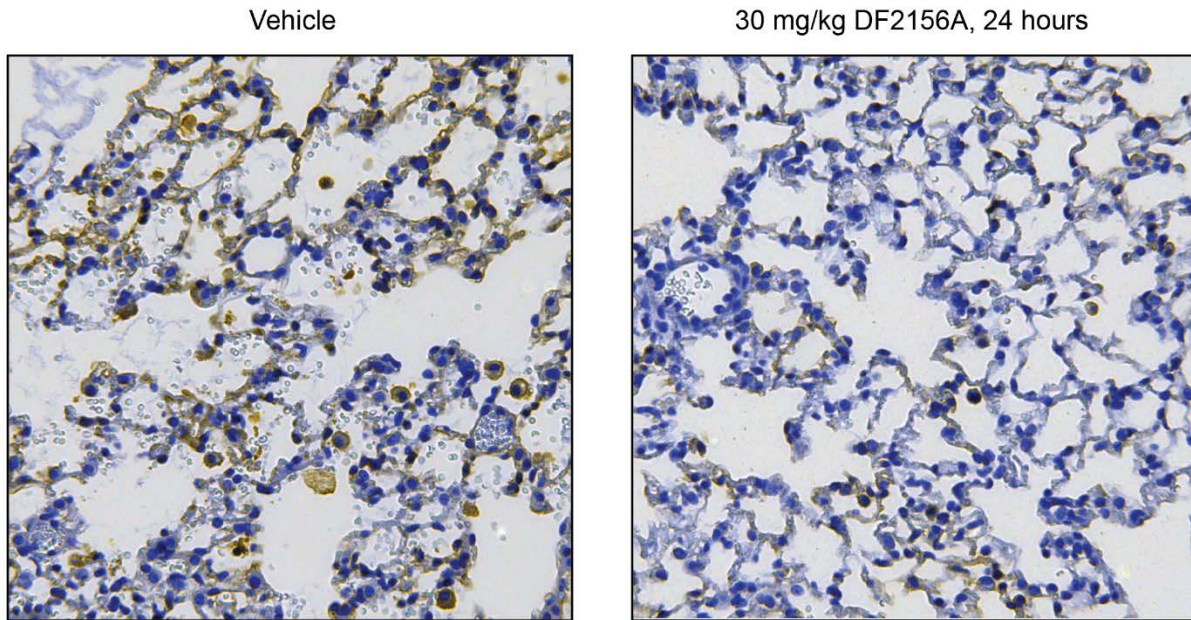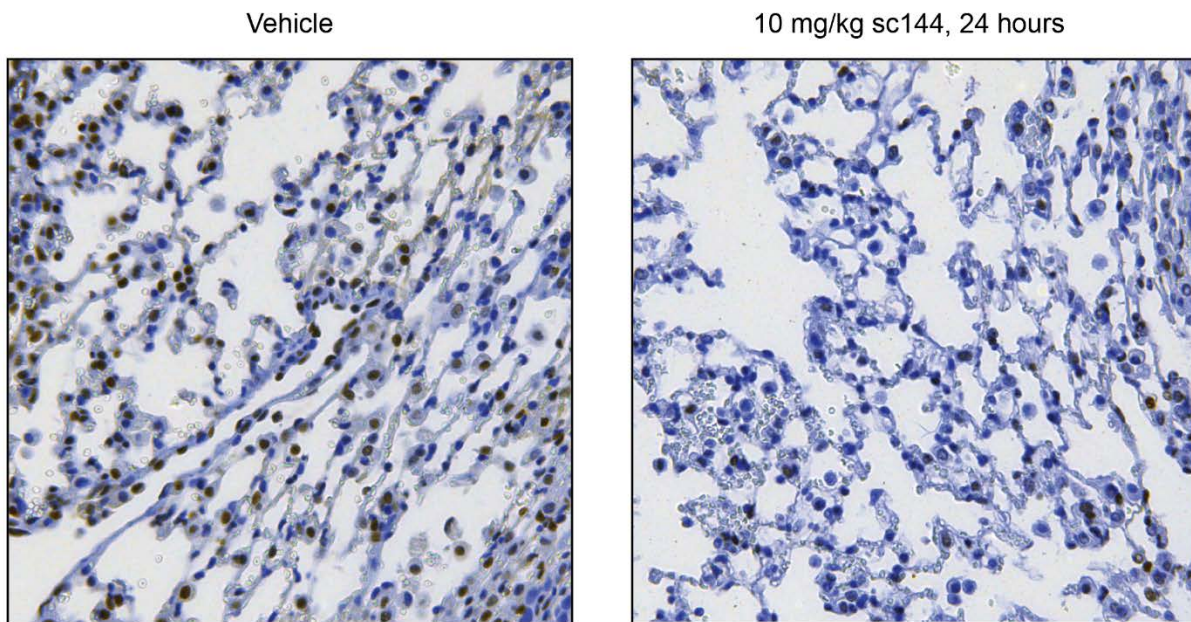
Brown = pSTAT3

Supplemental Figure 4. PD analysis in lung tissue of mice treated with DF2156A and sc144. Mice treated with injections of either DF2156A or SC144 daily were euthanized 24 hours subsequent to their 14th dose of drug. Lungs harvested from those mice were processed using standard FFPE, then sectioned and stained with IHC for either pFAK (downstream of

CXCL8) or pSTAT3 (downstream of IL6). Representative images are shown above. Receptor blockade reduced the amount of activation seen and the number of infiltrating cells, even at trough concentrations.
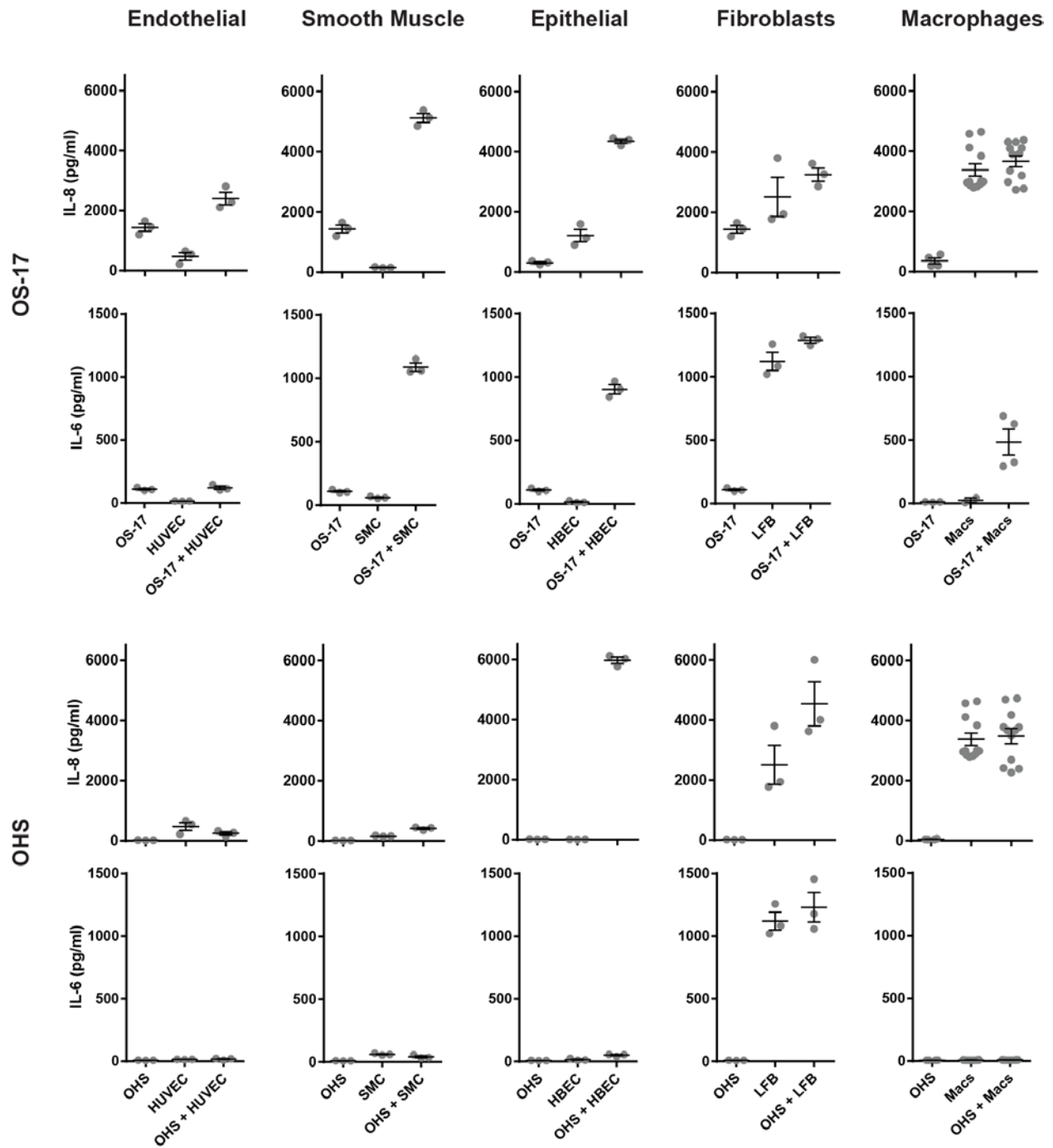
Supplemental Figure 5. Full panels of co-culture data evaluating for interactions that drive production of IL6 and CXCL8. OS cells (either OS-17 or OHS) were cultured alone or together with various primary human cell cultures: endothelial (human umbilical vein endothelial cells, HUVECs), lung smooth muscle cells (human bronchial smooth muscle cells, BSMCs),

lung epithelial cells (human bronchial epithelial cells, HBECs), lung fibroblasts (human lung fibroblasts), or macrophages (peripheral blood monocytes driven to early tissue macrophage phenotype as described in methods). Supernatants from each culture were subjected to ELISA for either IL6 or CXCL8.
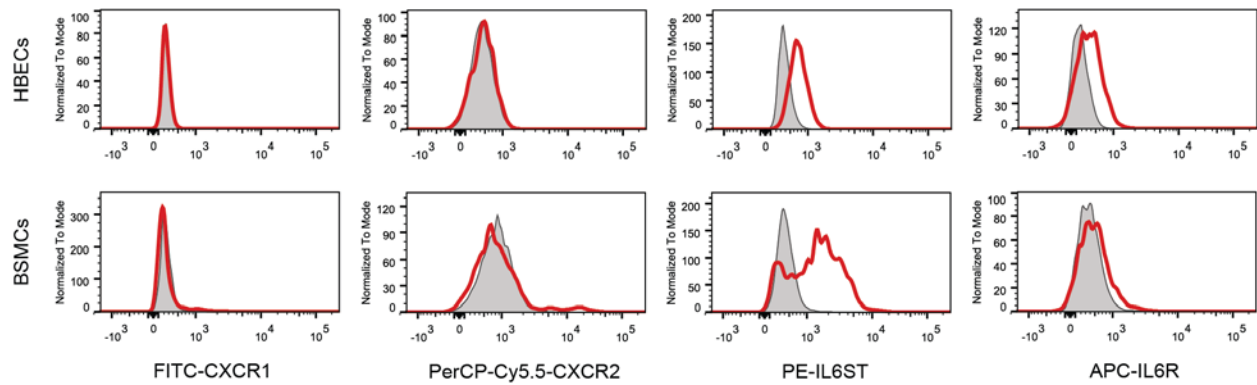
Supplemental Figure 6. Primary lung cells express receptors for IL6, while a small subset express receptors for CXCL8. Flow cytometry to evaluate for cell surface expression of the receptors for IL6 and CXCL8 on HBEC and BSMC. Both cell types express significant quantities of IL6 receptor components. A small subset of BSMCs expresses receptors for CXCL8, especially CXCR2.
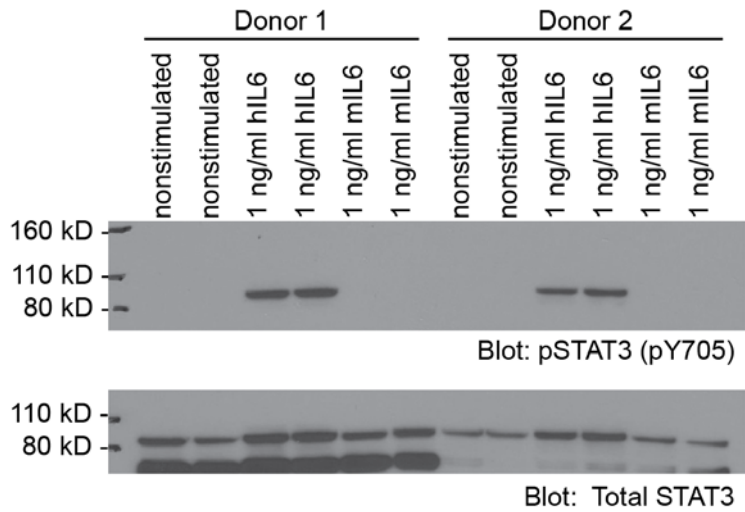
Supplemental Figure 7. Murine IL6 does not activate human receptors. Monocytes isolated from human blood (Miltenyi monocyte isolation kit, #130-096-537) were cultured in chemically defined hematopoietic media (Lonza X-VIVO, #BE02-060Q) supplemented with 10 ng/ml M-CSF for 72 hours, then starved in RPMI alone overnight. Wells were then treated with human or murine IL6 as noted above. 30 minutes after addition of cytokine, cells were lysed and harvested. Western blots were performed to evaluate for phospho- or total-STAT3 as noted.
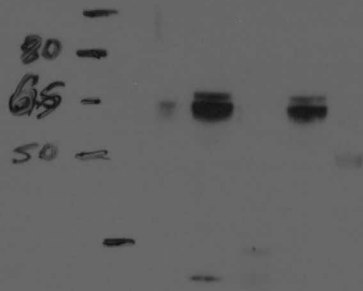
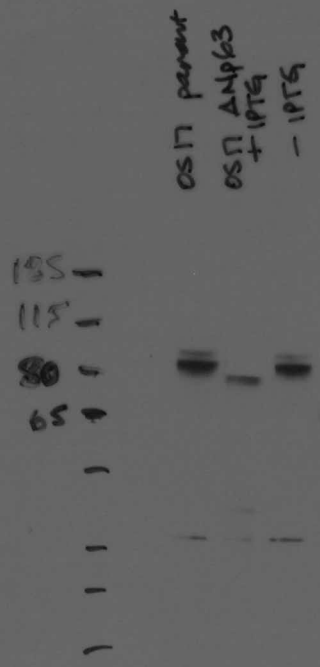Figure 6 deltaNp63

pSTAT3 Y705

osU present
osU ΔΝΔp63 + IPTG
- IPTG

195 —
115 —
80 —
65 —

Figure 6 pSTAT3 Y705
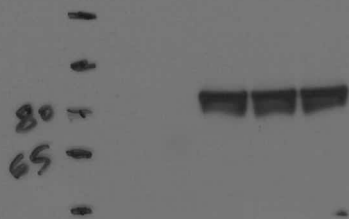
Figure 6 Total STAT3

β-actin

OSΠ parent
OSΠ ΔΝ + IPTG
- IPTG

65-
50-

30-
25-

Figure 6 beta actin

Supplemental Figure 7

Lane labels (top to bottom):
- Donor 21 - no treatment #1
- Donor 21 - no treatment #2
- Donor 21 - 1ng/mL h IL-6 #1
- Donor 21 - 1ng/mL h IL-6 #2
- Donor 21 - 1ng/mL m IL-6 #1
- Donor 21 - 1ng/mL m IL-6 #2
- Donor 29 - no treatment #1
- Donor 29 - no treatment #2
- Donor 29 - 1ng/mL h IL-6 #1
- Donor 29 - 1ng/mL h IL-6 #2
- Donor 29 - 1ng/mL m IL-6 #1
- Donor 29 - 1ng/mL m IL-6 #2

Molecular weight markers: 260, 160, 110, 80, 60, 50, 40, 30, 20, 15, 10

Notes:
- p-STAT3 at 1:4000
- anti-rabbit HRP at 1:4000
- 10 ug protein per sample

11-2-16

Donor 21- no txt #1
Donor 21- no txt #2
Donor 21 - 1ng/mL hIL-6 #1
Donor 21 - 1ng/mL hIL-6 #2
Donor 21 - 1ng/mL mIL-6 #1
Donor 21 - 1ng/mL mIL-6 #2
Donor 29- no txt #1
Donor 29- no txt #2
Donor 29- 1ng/mL hIL-6 #1
Donor 29- 1ng/mL hIL-6 #2
Donor 29- 1ng/mL mIL-6 #1
Donor 29- 1ng/mL mIL-6 #2

260 —
160 —

• STAT3 at 1:4000   110 —
                         80 —
• anti-rabbit HRP
   at 1:4000   60 —

                         50 —
                         40 —
• 10ug protein per
   sample   30 —
                         20 —

                         15 —
                         10 —